

Estimation of the boost converter inductance current in dynamic conditions by means of NARX neural network

Abstract. The article presents a method for estimating the Boost converter inductance current using a NARX neural network. The model works basing on selected sampled and calculated time series, without the involvement of any algebraic equations describing the circuit. The proposed solution enables the estimation of the current in static and dynamic states across the entire load range of the converter, as well as under dynamically changing levels of the supply voltage - this under closed loop output voltage control. The proposed approach can serve as a foundation for further work on the digital twin of the converter. All considerations are based on experimentally verified simulation model.

Streszczenie. W artykule przedstawiono sposób estymowania prądu indukcyjności przetwornicy typu Boost za pomocą sieci neuronowej typu NARX. Model działa w oparciu o wybrane szeregi czasowe spróbkowane i obliczone numerycznie, bez udziału jakichkolwiek równań algebraicznych opisujących układ. Zaproponowane rozwiązanie pozwala na wyznaczanie prądu zarówno w stanach statycznych jak i dynamicznych w pełnym zakresie obciążenia przetwornicy oraz przy zmieniających się dynamicznie poziomach napięcia zasilającego - to przy zamkniętej pętli regulacji napięcia wyjściowego. Zaproponowane rozwiązanie może służyć jako podstawa do dalszych prac nad bliźniakiem cyfrowym przedmiotowej przetwornicy. Wszystkie rozważania oparto na eksperymentalnie zweryfikowanym modelu symulacyjnym. (Estymacja prądu indukcyjności przetwornicy podwyższającej napięcie w stanach dynamicznych za pomocą sieci neuronowej NARX)

Keywords: boost converter, neural network, NARX, current estimator, digital twin
Słowa kluczowe: konwerter boost, sieć neuronowa, NARX, estymator prądu, bliźniak cyfrowy

Introduction

At this stage, data-driven models have well established position in the domain of power electronics. They do not only support faults detection and diagnostics but also serve as means for continuous circuits condition monitoring and predictive maintenance [1]. Moreover, data-driven models can be used for optimized control of power electronics systems where they deal with interactions between many power electronic circuits. By system data analysis, data-driven models can influence the system's control and protection settings to maintain its efficiency and stability under different operating conditions. Such models can also be combined with digital twins being digital replicas of physical circuits, [2], to create a more comprehensive and accurate representation of power electronic circuits and systems [3].

Keeping that in mind, a data-driven model basing on NARX neural network type, NARX-NN, has been developed for calculation of current flowing through inductance of the Boost converter - this under closed loop output voltage PI control. It works basing on selected sampled and calculated time series, without the involvement of any algebraic equations describing the circuit. Developed solution enables estimation of the current in static and dynamic conditions across the entire load range of the converter, as well as under dynamically changing supply voltage. Performance during the transients is of particular importance here, [4]. The proposed approach can serve as a foundation for further works leading towards a digital twin of not only such simple converters but more advanced topologies. Having such digital twins will lead towards new dimension of diagnostics and prognostics of power converters in future power systems.

All works, for simplicity reasons, have been done with the converter modelled in Matlab-Simulink environment. The model has been developed with the key parasitic components taken into account, see Fig. 1, according to experience gained in the past, [5].

In this paper details on the circuit and its model are given in section entitled Boost converter simulation model as a source of time series data. This is followed by Selection of the NARX-NN model data, where we discuss the model input vector details. After that, in section Selection of the NARX-NN model hyper-parameters and its training at fixed input voltage and variable load, details on single NN-model

configuration, training and performance are given. As next, we investigate Effect of the input voltage variation on the single model performance. This leads to Model topology for variable input voltage and load, where few NARX-NN models are combined together to deal with the input voltage variation. Finally, we conclude the paper and discuss future research directions in the last section.

Boost converter simulation model as a source of time series data

For simplicity reasons, a simulation model of a boost converter circuit with additional parasitic components, see Fig. 1, has been used to generate time series used for the NN inductance current estimator development. The circuit parameters are listed in the Table 1.

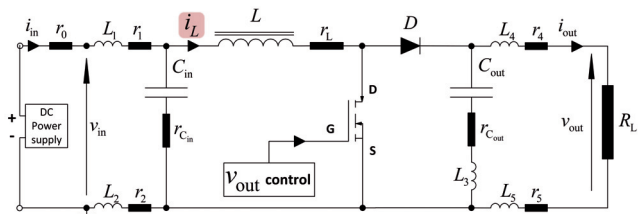


Fig. 1. A Boost converter circuit with selected parasitic components and control circuit block. The control is basing on classical closed loop v_{out} regulation with PI controller, where gains $K_P = 0.0008 \text{ 1/V}$ and $K_I = 0.8 \text{ 1/V.s}$ are used.

The signals have been sampled with sampling frequency, $f_{A2D} = 250 \text{ kHz}$, equal 10 times the Pulse With Modulation frequency, f_{PWM} . The ratio of 10 has been experimentally proven to be sufficient for satisfactory preservation of information about the circuit dynamics within single PWM cycle. The additional inductances and resistances indexed 0..5 have been added to better emulate behaviour of the real world circuit operation. In addition to the extra parasitics, random noise at level of the two Least Significant Bits, LSB, has been included at the signals sampling stage. The signals have been sampled with 12 (currents) and 16 (voltages) bits resolution which is driven by an experimental setup used at stage of the sampling frequency investigation. This of course does not impede use of lower resolutions dictated by the closed loop control circuits, say 12 or less bits. In such cases normally the count of unstable bits decreases.

As expected, the simulation model provided us with cost

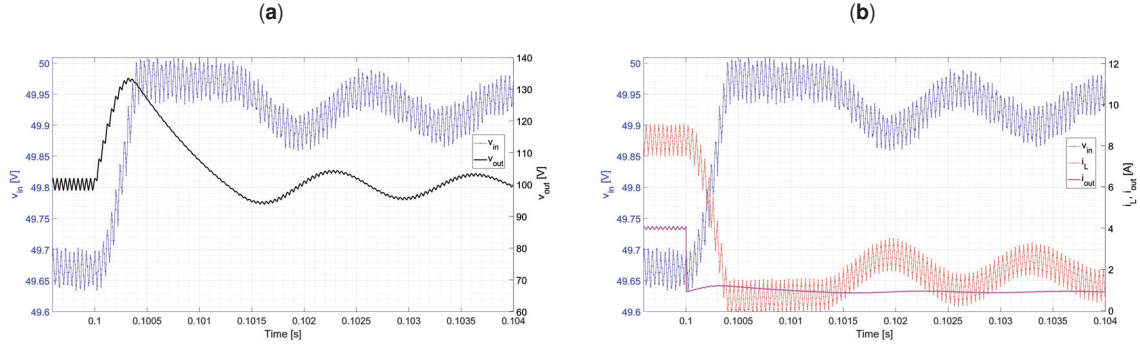


Fig. 2. Selected Boost converter time series sampled with 250kHz: (a) voltages and (b) voltages and currents. They are based on a circuit configuration shown in Fig. 1, with settings according to Table 1.

effectiveness and easiness during selection of suitable time series. Selected simulation results can be seen in Fig. 2, where the input voltage, v_{in} , can be seen together with the output voltage, v_{out} , and inductance and output currents, i_L and i_{out} , respectively. They are in steady- and transient-states.

Selection of the NARX-NN model data

Input vector according to Eq. 1 has been used as a carrier of information about the converter states needed to estimate the inductance current under closed loop output voltage PI control. Here the current is estimated at fixed DC power supply voltage which varies at the Boost converter input according to the parasitic resistance r_0 .

$$(1) \quad \mathbf{u}_{(k)} = \begin{bmatrix} v_{outError}(k) \\ t_{on}(k) \\ clk4TPWM(k) \\ rd_{vin2iout}(k) \\ \Delta rd_{vin2iout}(k) \\ \frac{dd(k)}{dt_{A2D}(k)} \end{bmatrix}$$

where: $v_{outError}(k)$ is the output voltage error in [V]; $t_{on}(k)$ is the on-time within the switching period in [s]; $clk4TPWM(k)$ is a clock-like signal in form of linear slope in range 0..1 within each PWM cycle; $rd_{vin2iout}(k)$ is a dynamic resistance calculated as $\frac{v_{in}(k)}{i_{out}(k)}$ in [Ω]; $\Delta rd_{vin2iout}(k)$ is change of the $rd_{vin2iout}(k)$ between two consecutive sampling periods in [Ω]; $\frac{dd(k)}{dt_{A2D}(k)}$ is a derivative of the duty cycle $d(k)$ in respect to the sampling time $t_{A2D}(k)$ - the value is kept const till the duty cycle next change. All the components of Eq. 1 are calculated in reference to the sampling time $t_{A2D}(k)$.

In addition to the $\mathbf{u}_{(k)}$, delayed values of the model output $\tilde{\mathbf{y}}_{(k)} = [\tilde{i}_L(k)]$ are used as the NARX topology requires, see Fig. 3.

The $\mathbf{u}_{(k)}$ is mostly based on signals normally used in such a circuit working in a system under digital control or supervision. They are normally needed in a control loop (or loops) or at a protection stage but of course at lower sampling rate. Additionally calculated are only derivative of the duty cycle, $\frac{dd(k)}{dt_{A2D}(k)}$, and synchronization clock $clk4TPWM(k)$. They have proven to be useful during the $\tilde{i}_L(k)$ calculation under the closed loop control, Fig. 1. Some of the $\mathbf{u}_{(k)}$ components have been selected basing on correlation analysis of the circuit data. Nevertheless, not all of them. The rest have been chosen basing on authors experience and experiments. Example correlations analysis results can be seen in Fig. 4.

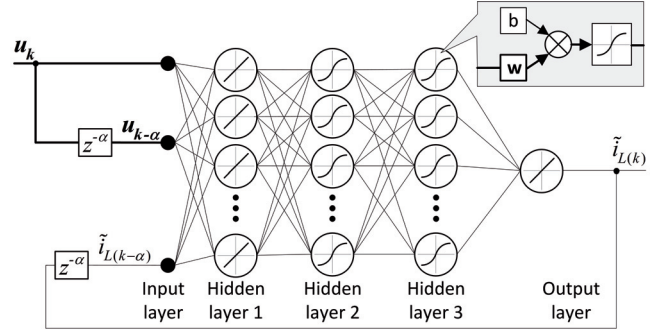


Fig. 3. NARX-NN i_L model concept. It is based on three hidden, fully connected layers with 13 neurons each, 3×13 , and input vector, $\mathbf{u}_{(k)}$, according to Eq. 1. Different α -delays are listed in Table 2.

The correlation, as measure of similarity between analysed time series, informs in quantitative way about level of change of one series in relation to the other. If it is equal to 1 then the two compared signals have the same character. This can be seen in the matrix diagonal. If it is equal to -1 then the signals are opposite as can be seen in case of the $v_{out}(k)$ and $v_{outError}(k)$. Here, it is worth to emphasize that we have no simple recommendation regarding desired correlation level as a criterion for signals selection in case of circuits with closed loop control. At this stage, one general observation may be that a variety of levels may contribute to better results. Nevertheless, it may be desirable to balance higher correlations, say around 0.9, by lower ones, say below 0.4.

In addition to the above input vectors $\mathbf{u}_{(k)}$ and $\tilde{\mathbf{y}}_{(k)} = [\tilde{i}_L(k)]$, the inductance current as the circuit output vector is used as a reference at the model training stage.

$$(2) \quad \mathbf{y}_{(k)} = [i_L(k)]$$

The $\mathbf{y}_{(k)}$ is also used for the model quality assessment by means of its comparison with the model output $\tilde{\mathbf{y}}_{(k)} = [\tilde{i}_L(k)]$ according to equation Eq. 3 discussed later in the text.

Selection of the NARX-NN model hyper-parameters and its training at fixed input voltage and variable load, $\tilde{i}_L = f(i_{out})$

A NARX-NN with three hidden layers, as shown in Fig. 3, has been used. The model input consists of the $\mathbf{u}_{(k)}$ and the $\tilde{\mathbf{y}}_{(k)}$ delayed according to α listed in Table 2. The delays are not the same for all time series. They have been selected experimentally for the best model performance. Each of fully connected hidden layers consists of 13 neurons with activation functions as shown in Fig. 3. The functions and neurons count have been selected experimentally too.

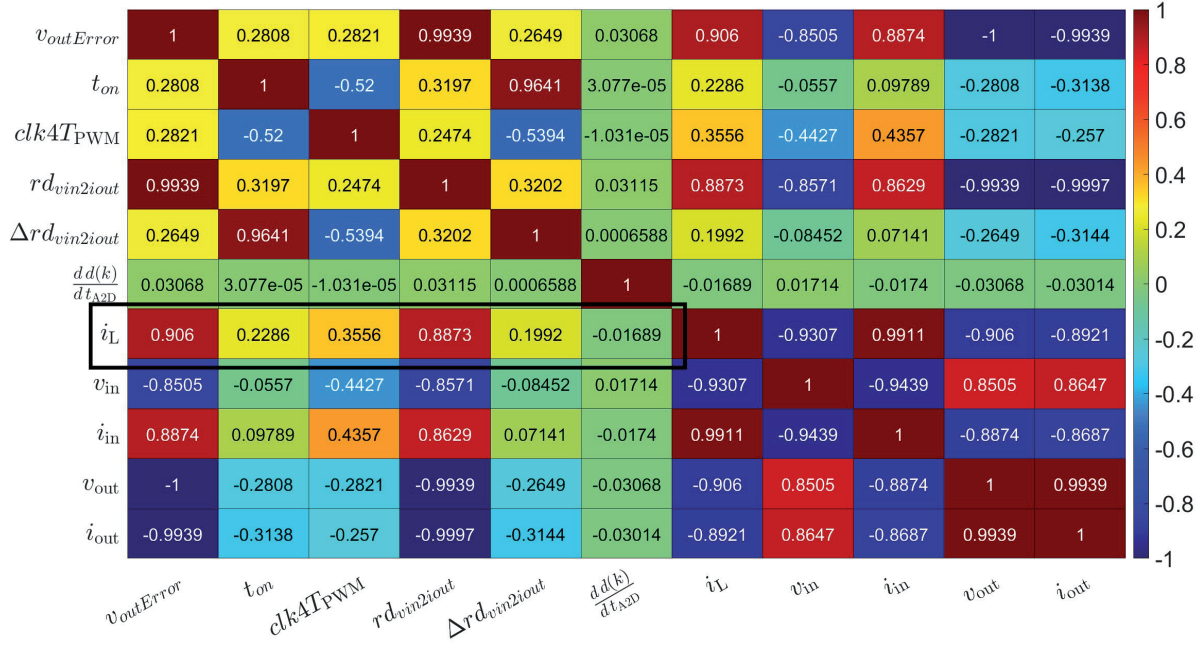


Fig. 4. Correlations between selected sampled and calculated boost converter time series. The black rectangle indicates the input vector $\mathbf{u}_{(k)}$ components according to Eq. 1.

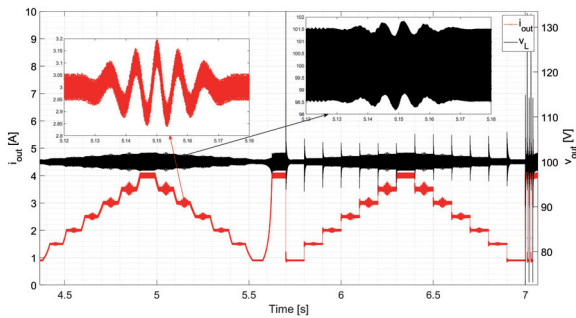


Fig. 5. Profile of the output current i_{out} used to shape the i_L as the training data set. Corresponding output voltage seen by the closed loop PI control is described in the right axis. The sinusoidal parts allow for introduction of additional requirements to the training process.

The model has been trained in Matlab with the *train* function. The training was done in the open loop NARX configuration. Trained network had been closed with the *closeloop* function. Inductance current corresponding to the load current profile in format shown in Fig. 5 was used for training of the model. Such profile has provided sufficient amount of freedom in shaping the dynamics of the model in presence of variable load current under closed loop output voltage control. Example static and dynamic performance of trained model can be seen in Fig. 6. The results are for fixed DC power supply voltage. Summed absolute error, according to Eq. 3, in time from 0.005..0.025s is 61.676A. The time corresponds to k -samples from 1250 to 6250.

$$(3) \quad i_{L,error}^{est} = \sum_{k=1250}^{6250} \tilde{i}_L(k) - i_L(k)$$

The error does not take into account initial time of the model convergence. One can see that the maximum estimated inductance current absolute error during transient related to maximum step change in the output current is less

than 0.4A which corresponds to 5%. This may call for further improvements, even if it takes less than 3 PWM cycles, especially if the NARX-NN model is to be used as a support of control loops. Rest of the transient errors is below 1.25% which makes the model a good starting point for development of purely data-driven digital twin of the Boost converter. It must be emphasised here that the model sensitivity to the circuit parameters tolerance and variations is to be addressed in future works. Nevertheless, it has been observed that up to $\pm 10\%$ variations in the input or output capacitances or the main inductance do not cause serious deterioration in the model performance. Combinations of the variations are still to be investigated.

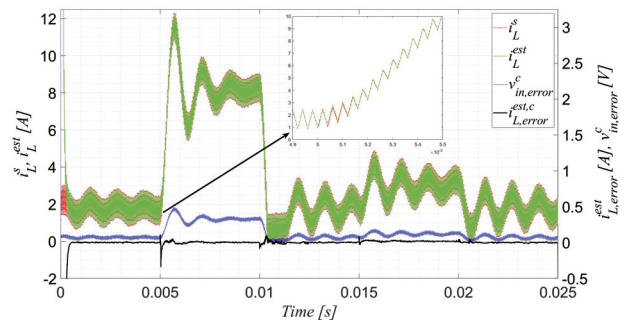


Fig. 6. NARX-NN \tilde{i}_L model, Fig 3, results in presence of the load current, i_{out} , step changes according to amplitudes $\{0.9; 4; 0.9; 1.5; 0.9\}$ A. The DC power supply voltage was constant, equal to 50V. The real input voltage variation calculated at the terminals of the converter can be seen as v_{in}^c . The $i_{L,error}^{est}$ stands for difference between the sampled inductance current, i_L^s , and the model estimated values, i_L^{est} . Cumulated the absolute error in time of 0.005..0.025s is 61.676A.

Effect of the input voltage variation on the single model performance

Model shown in Fig. 3 has been tested with variable DC power supply output voltage. Selected results can be seen in Fig. 7. There is clear degradation of the performance when compared to results from Fig. 6. The calculated error is equal

to 497.137A and is eight times bigger. In such case decision about training of dedicated models at different fixed DC power supply voltage levels has been made. The models configuration and development path are exactly the same as described in the previous section.

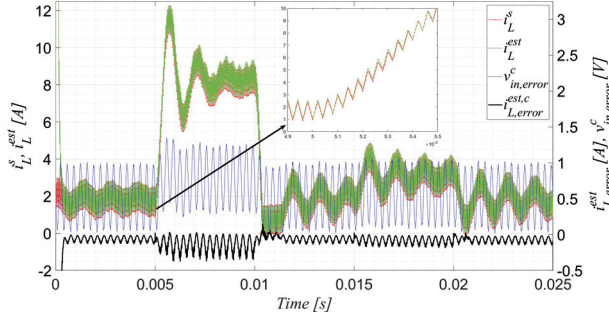


Fig. 7. NARX-NN \tilde{i}_L model, Fig 3, results in presence of the load current, i_{out} , step changes according to amplitudes $\{0.9; 4; 0.9; 1.5; 0.9\}A$. The DC power supply voltage was changing around DC point equal to 49.45V with frequency of 3kHz and amplitude of 0.45V. The real input voltage variation calculated at the terminals of the converter can be seen as $v_{in,error}^c$. Cumulated the absolute error $i_{L,error}^{est}$ in time, 0.005..0.025s is 497.137A.

Model topology for variable input voltage and load, $\tilde{i}_L = f(v_{in}, i_{out})$

Having number of NARX-NN models developed at different DC power supply output voltages it was necessary to combine them somehow in one model. One of the simplest solutions has been selected. They have been coupled as shown in Fig. 8. It has been done by means of triangular membership functions. Initially it has been decided to split the models by 0.2VDC. Selection of optimum models split in terms of the DC input voltage distance is still a subject to further research. Obtained results can be seen in Fig. 9. In this case the error is equal to 242.547A and is less than 4 times of the single model shown in Fig. 3. Further improvements can be made by more advanced models coupling methods, which is a subject to our further research.

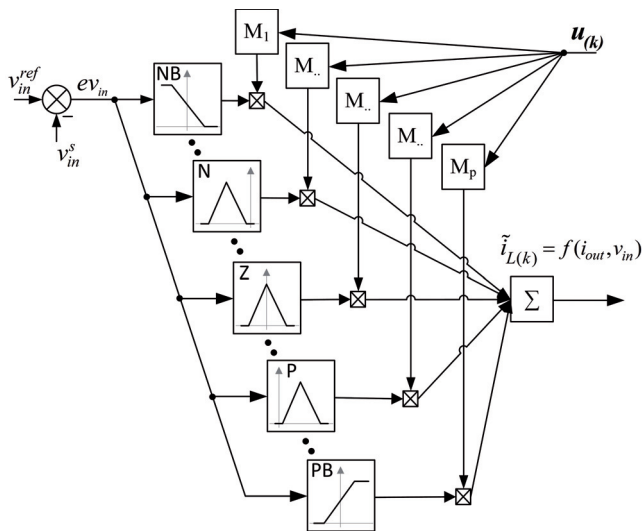


Fig. 8. NARX-NN model used for the \tilde{i}_L calculation in presence of variable DC power supply voltage. The model is based on the triangular membership functions with the base points shifted by $\pm 0.2V$ from the peak location.

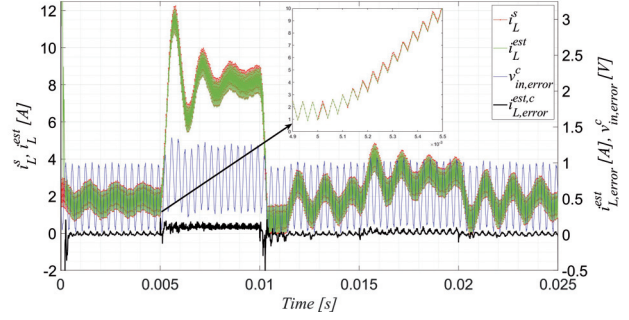


Fig. 9. Combined NARX-NN \tilde{i}_L model, Fig 8, results in presence of the load current, i_{out} , step changes according to amplitudes $\{0.9; 4; 0.9; 1.5; 0.9\}A$. The DC power supply voltage was changing around DC point as in case of Fig. 7. Cumulated the absolute error $i_{L,error}^{est}$ in time, 0.005..0.025s is 242.547A.

Table 1. Parameters of the Boost converter model

Parameter	Value
Input rated voltage, V_{in}^{rtd}	50 VDC
Output rated voltage, V_{out}^{rtd}	100 VDC
Rated output power, P_{out}^{rtd}	250 W
Maximum output power, P_{out}^{max}	400 W
Equivalent DC supply resist. r_0	40 mΩ
Nominal input capacitance, C_{in}	20 μF
Equivalent serial resist. of C_{in} , $r_{C_{in}}$	10 mΩ
Converter inductance, L	650 μH
Equivalent series resistance of L , r_L	6 mΩ
N-Channel MOSFET R_{DSon}	75 mΩ
N-Channel MOSFET input capacitance, C_{iss}	1350 pF
N-Channel MOSFET transfer capacitance, C_{rss}	3 pF
N-Channel MOSFET output capacitance, C_{oss}	58 pF
Diode forward voltage, v_{DF}	0.375 V
Diode On-resistance, R_{Don}	200 mΩ
Nominal output capacitance, C_{out}	20 μF
Equivalent serial resist. of C_{out} , $r_{C_{out}}$	10 mΩ
Switching frequency, f_{PWM}	25 kHz
Sampling frequency A2D, f_{A2D}	250 kHz
A2D resolution for currents, res_i	12 bit
A2D resolution for voltage, res_v	16 bit
Signals processing frequency, f_p	250 kHz
Model inductance, L_1	2 nH
Model resistance, R_1	10 μΩ
Model inductance, L_2	0.25 nH
Model resistance, R_2	10 μΩ
Model inductance, L_3	2 nH
Model inductance, L_4	100 nH
Model resistance, R_4	10 μΩ
Model inductance, L_5	100 nH
Model resistance, R_5	10 μΩ

Table 2. Delays of the NARX-NN model of \tilde{i}_L

Parameter	Values of α in cycles
$v_{outError}(k)$	1:1:3
$t_{on}(k)$	1:1:3
$clk4T_{PWM}(k)$	1:1:5
$rd_{vin2iout}(k)$	1:1:5
$\Delta rd_{vin2iout}(k)$	1:1:5
$\frac{d d(k)}{d t_{A2D}(k)}$	1:10:10
$Y(k)$	1:1:3

Conclusions

NARX–NN model solution for estimation of the Boost converter inductance current has been proposed in this paper. The model has been developed for the converter operating in full load range under closed loop output voltage control with a PI compensator.

The model is purely data–driven, without algebraic equations describing operation of the circuit. The data in form of time series has been generated from a trusted simulation model which takes into account key parasitic components and sampling noise present in a real circuit.

Operation of the model has been investigated under constant and variable DC power supply voltage supplying the converter. For purpose of operation under variable input voltage a combined model has been recommended.

Presented solution constitutes strong foundation for further works leading towards development of a digital twin of the Boost converter.

Acknowledgment

Majority of calculations have been carried out using resources provided by Wrocław Centre for Networking and Supercomputing (<https://wcss.pl>), under grant name *runnerOne*.

Authors: *Radosław Nalepa DSc, Karol Najdek DSc, Division of Power Networks and Systems, Department of Electrical Power Engineering, Faculty of Electrical Engineering, Wrocław University of Science and Technology, Wybrzeże Wyspiańskiego 27, 50-370 Wrocław, Poland, email: radoslaw.nalepa@pwr.edu.pl*

REFERENCES

- [1] Y. Peng, S. Zhao and H. Wang: A Digital Twin Based Estimation Method for Health Indicators of DC–DC Converters, *IEEE Trans. on Power Electronics*, 36, pp. 2105–2118, 2021.
- [2] M. M. Rathore, S. A. Shah, D. Shukla, E. Bentafat and S. Bakiras.: The Role of AI, Machine Learning, and Big Data in Digital Twinning: A Systematic Literature Review, Challenges, and Opportunities, *IEEE Access* 2021 Vol. 9, pp. 32030-32052, 2021.
- [3] M. Grieves and J. Vickers.: *Digital Twin: Mitigating Unpredictable, Undesirable Emergent Behavior in Complex Systems*, Springer International Publishing, 2017.
- [4] A. Wunderlich and E. Santi.: Digital Twin Models of Power Electronic Converters Using Dynamic Neural Networks, *IEEE Applied Power Electronics Conference and Exposition (APEC)* 14-17 June 2021, pp. 2369-2376 , 2021.
- [5] R. Nalepa, K. Najdek and B. Strong: Hybrid Tuning of a Boost Converter PI Voltage Compensator by Means of the Genetic Algorithm and the D-Decomposition, *MDPI Energies* 2021 Vol. 14 Issue 1, pp. 1-20 , 2021.
- [6] R. W. Erickson and D. Maksimović: *Fundamentals of Power Electronics*, second edition, Kluwer Academic Publishers, 2024.